Journal of Adaptive Learning Technologies
ISSN **2997-3902** (Online)
Vol. 3, No. 3, March 2026,
Available online at: https://scientificbulletin.com/index.php/JALT

Article

Electrochemical Investigation of the Corrosion Inhibition Efficiency of the Supramolecular Complex B-Sdofda for N20 Steel

Ilyos Askarovich Eliboev[1], Diyorbek Qahramon o'g'li Jumabekov[2]
[1]PhD, Samarkand State Pedagogical Institute, Republic of Uzbekistan, Samarkand
[2]Samarkand State Pedagogical Institute, Republic of Uzbekistan, Samarkand. Master's Student

Article information:
Manuscript received: 13 February 2026; **Accepted:** 14 March 2026; **Published:** 19 April 2026

Abstract: This study presents the results of electrochemical investigations on the anticorrosion efficiency of the supramolecular complex beta-cyclodextrin–orthophenylenediamine (β–SDOFDA) for N20 steel. The inhibitory properties of β–SDOFDA were examined using potentiodynamic polarization and electrochemical impedance spectroscopy methods. Based on the obtained data, key parameters such as corrosion current density, corrosion potential, inhibition efficiency, double-layer capacitance, charge transfer resistance, constant phase element parameters, and the average surface roughness of the metal were determined. The results demonstrated that the selected inhibitor effectively protects the metal surface against corrosion.

Keywords: Electrochemistry, Potentiodynamic Polarization, Tafel Curves, Electrochemical Impedance Spectroscopy, N20 Steel, Beta-Cyclodextrin (B–SD), Orthophenylenediamine (OFDA).

1. Introduction

Corrosion inhibitors are adsorbed onto metal surfaces, forming a stable and protective thin film. Both chemical and physical adsorption mechanisms are considered the most favorable for inhibitor adsorption and the formation of a protective layer [1]. The formation of a stable protective film at the interface between the metal surface and the solution effectively isolates the corrosion process. As a result, the influence of ions, water molecules, and oxygen on the metal surface is significantly reduced [2].

It has been established that compounds based on beta-cyclodextrin are stable and environmentally friendly corrosion inhibitors. In general, β-CD derivatives contain a higher number of nitrogen atoms, which are prone to protonation. Physical adsorption occurs due to electrostatic interactions between the positively charged nitrogen atoms of the inhibitor and the negatively charged metal surface [3].

On the other hand, the inhibitor is adsorbed onto the metal surface through the formation of strong covalent bonds. This is attributed to the presence of electron-rich heteroatoms, functional groups, and aromatic rings in these compounds, which facilitate chemical interactions between the corrosion inhibitor and the metal surface. Electron pairs from the inhibitor are transferred to the vacant d-orbitals of the metal, resulting in the formation of strong chemical bonds [4].

β-SD is a macrocyclic oligomer with an external diameter of 7.8 Å, a cavity diameter of 6.5 Å, a cone height of 7.8 Å, and a cavity volume of 25.35 Å^3, consisting of seven glycosidic units. It possesses a truncated cone-shaped structure with a hydrophilic outer

surface and a hydrophobic inner cavity. During the formation of supramolecular complexes, this cavity enables the inclusion of guest molecules [5].

Using techniques such as infrared spectroscopy (IR), differential scanning calorimetry (DSC), scanning electron microscopy (SEM), X-ray diffraction (XRD), and proton nuclear magnetic resonance (^{1}H NMR), it has been confirmed that the hydrophobic cavity of β-SD can form host–guest complexes and facilitate the encapsulation of organic compounds. In particular, β-SD also enhances the anticorrosion properties of other compounds [6].

β-SD has a non-hygroscopic, homogeneous, crystalline molecular structure and consists of seven D-glucose units linked by α-(1→4) glycosidic bonds [7]. The lone electron pairs of the glycosidic oxygen bridges are oriented toward the interior of the cavity, indicating a high electron density and Lewis base character. These properties suggest that the inner surface of β-SD is hydrophobic, in contrast to its hydrophilic outer surface [8].

The primary hydroxyl groups (attached to glucose units via –CH_2) and secondary hydroxyl groups (directly bonded to glucose units) located on the outer surface of β-SD enhance its water solubility [9]. Although hydroxyl groups are present on both the inner and outer surfaces, the internal cavity of β-SD remains hydrophobic, while the external surface is hydrophilic [10].

Modifications of β-SD-based nanomaterials and polymers occur through reactions between the external hydroxyl groups of β-SD and the carboxyl groups of substrates [11]. The inhibitory properties of β-SD can be further improved by chemical modification of the –OH groups on its outer rings [12].

2. Materials and Methods

The selection of N20 steel in this study is обусловлен its widespread use as a primary material for metal pipes in oil and gas transportation [13]. The protection of N20 steel against corrosion is a relevant issue in materials science, chemistry, and engineering. It belongs to the class of carbon steels [14]. The chemical composition of N20 steel is as follows: Fe ~98%, Cr ≤0.25%, Cu ≤0.30%, Ni ≤0.30%, Mn 0.35–0.65%, As 0.08%, Si 0.17–0.37%, C 0.17–0.24%, P ≤0.035%, and S ≤0.040% [6;7].

Prior to the experiments, the metal samples were mechanically cleaned and polished using abrasive papers of varying grit sizes (from 400 to 1200), resulting in a clean and smooth surface [15]. The prepared metal specimens were then rinsed three times with distilled water and ethanol. Subsequently, they were degreased with acetone and air-dried [16].

All electrochemical experiments were carried out in 0.5 M hydrochloric acid (HCl) solutions at temperatures of 303, 313, 323, and 333 K. The selected strongly acidic and aggressive medium has significant practical relevance, as highly concentrated acid solutions are commonly used for cleaning N20 steel pipelines [17]. Therefore, a 0.5 M HCl solution was chosen as the test medium. The solutions were prepared in accordance with international standards using reagents of appropriate purity [18].

For the experimental studies, corrosion inhibitors were used at concentrations ranging from 25 to 100 mg/L.

Electrochemical Methods.

Electrochemical studies were carried out in a three-electrode electrochemical cell consisting of a platinum plate electrode (counter electrode), a saturated calomel electrode (reference electrode), and a working electrode (N20 steel specimen with dimensions of 2 × 1 cm). The electrochemical experiments were performed using a CORRTEST instrument (model CS310, Wuhan, China). Electrochemical data processing and calculations were conducted using CS Studio software (Wuhan, China) [19].

Potentiodynamic Polarization Method.

In the potentiodynamic polarization (PDP) study, a potential scan range of ±0.250 V was applied at a scan rate of 1 mV/s [20]. The electrochemical protection efficiency (η_PDP) was determined as the difference between the corrosion current density of the system without the inhibitor and that with the inhibitor (see Equation 1).

$$\eta_{PDQ}, \% = \frac{i^{o}_{korr} - i^{i}_{korr}}{i^{o}_{korr}} \times 100 \quad (1)$$

3. Results and Discussion

Effect of β-SDOFDA on the Electrochemical Corrosion Processes. The effect of the inhibitor on corrosion processes, such as hydrogen evolution at the cathode and metal dissolution into cations at the anode, was investigated using the potentiodynamic polarization method. This method is based on Tafel curves obtained for solutions with and without the β-SDOFDA inhibitor in 0.5 M hydrochloric acid (with N20 steel as the working electrode) (see Fig. 1), as well as on the values of various electrochemical parameters (see Table 1).

Based on the obtained results, the following conclusions were drawn:

(I) It is evident that the Tafel curves shift toward regions of higher corrosion current density (i_corr) in uninhibited systems. With the formation of a protective layer due to inhibition, the Tafel curves shift toward lower current density values (i_corr) as a result of a significant increase in polarization resistance. This shift becomes more pronounced with increasing inhibitor concentration. The decrease in i_corr indicates the strength and effectiveness of the protective layers formed on the metal surface. This protective layer shields the metal surface from the corrosive environment, thereby preventing corrosion [21].

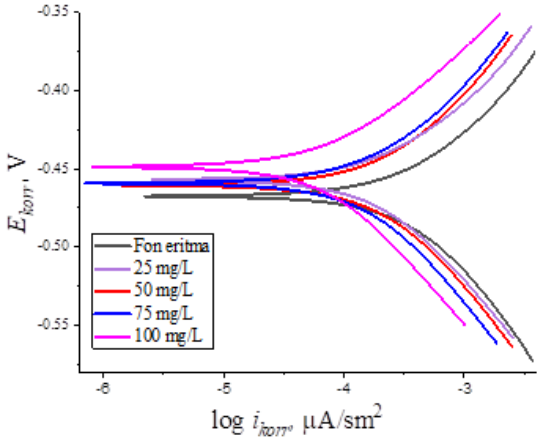

Figure 1. Tafel curves for N20 steel working electrode in 0.5 M HCl solution with and without the β-SDOFDA inhibitor.

(II) The difference between the corrosion potentials (E_corr) of the inhibited and uninhibited systems is less than 40 mV, indicating a mixed-type adsorption of β-SDOFDA on the metal surface.

(III) The corrosion current density (i_corr) values for the uninhibited system are in the μA/cm² range, indicating a very high corrosion rate. Upon the addition of β-SDOFDA, this value decreased to 0.85 μA/cm². Based on these values, the corrosion inhibition efficiency was calculated to be 93.38%.

(IV) The Tafel polarization curves (β_a, β_c) shifted in both anodic and cathodic directions upon the addition of the β-SDOFDA inhibitor, indicating a reduction in the corrosion rate due to polarization processes associated with the formation of a protective layer.

(V) The uninhibited metal surface undergoes a high corrosion rate in a highly polarized solution, which is attributed to the low polarization resistance of the metal surface. In contrast, in the presence of the β-SDOFDA inhibitor, the polarization resistance increases significantly due to the formation of protective films on the metal surface [22].

Table 1. Calculated electrochemical parameter values for solutions with and without the β-SDOFDA inhibitor in 0.5 M hydrochloric acid (N20 steel working electrode).

Parameters	C_{ing}, mg/l				
	Phon	25	50	75	100
i_{korr}, μA/sm²	12,85	1,87	1,65	1,03	0,85
E_{korr}, mV	-479	-456	-459	-461	-452
β_a, mV	275,6	251,9	234,1	201,5	185,6
$-\beta_k$, mV	230,9	221,7	201,5	184,1	152,6
η_{PDQ}, %	-	85,44	87,15	91,98	93,38

Tafel curves for solutions with and without the β-SDOFDA inhibitor. Since β-SDOFDA exhibits good hydrophobic properties, the interaction between the metal surface and water molecules is significantly reduced. This also leads to an increase in polarization resistance. As a result, a protective layer is formed due to the replacement of water molecules on the metal surface by β-SDOFDA.

4. Conclusion

Electrochemical studies based on potentiodynamic polarization lead to the following conclusions:

1. During the complexation of iron ions in N20 steel with β-SDOFDA and upon the introduction of the inhibitor into the corrosive medium, a decrease in entropy values was observed due to adsorption on the metal surface;
2. The corrosion inhibition efficiency reached 93.38%. The corrosion current density (i_corr) for the uninhibited system, which was 12.85 μA/cm², decreased to 0.85 μA/cm² in the presence of β-SDOFDA;
3. Compared to the uninhibited solution, characterized by low polarization resistance of the metal surface, a significant increase in polarization resistance was observed in the presence of the β-SDOFDA inhibitor due to the formation of protective layers.

REFERENCES

[1] B. Fan, G. Wei, Z. Zhang, and N. Qiao, "Characterization of a supramolecular complex based on octadecylamine and β-cyclodextrin and its corrosion inhibition properties in condensate water," *Corros. Sci.*, vol. 83, pp. 75–85, 2014.

[2] A. Dehghani, G. Bahlakeh, B. Ramezanzadeh, A. H. J. Mofidabadi, and A. H. Mostafatabar, "Benzimidazole loaded β-cyclodextrin as a novel anti-corrosion system: Coupled experimental/computational assessments," *J. Colloid Interface Sci.*, vol. 603, pp. 716–727, 2021.

[3] A. Dehghani, G. Bahlakeh, B. Ramezanzadeh, and A. H. J. Mofidabadi, "Electronic DFT-D modeling of L-citrulline molecules interactions with Beta-CD aligned rGO-APTES multifunctional nanocapsule for anti-corrosion application," *J. Mol. Liq.*, vol. 354, p. 118814, 2022.

[4] E. Berdimurodov *et al.*, "Green β-cyclodextrin-based corrosion inhibitors: Recent developments, innovations and future opportunities," *Carbohydr. Polym.*, p. 119719, 2022.
[5] Y. Cao *et al.*, "Green corrosion inhibitor of β-cyclodextrin modified xanthan gum for X80 steel in 1 M H_2SO_4 at different temperature," *J. Mol. Liq.*, vol. 341, p. 117391, 2021.
[6] L. Guo *et al.*, "Eco-friendly food spice 2-furfurylthio-3-methylpyrazine as an excellent inhibitor for copper corrosion in sulfuric acid medium," *J. Mol. Liq.*, vol. 317, p. 113915, 2020.
[7] D. K. Verma *et al.*, "Experimental and computational studies on hydroxamic acids as environmentally friendly chelating corrosion inhibitors for mild steel in aqueous acidic medium," *J. Mol. Liq.*, vol. 314, p. 113651, 2020.
[8] E. Berdimurodov *et al.*, "Novel cucurbit[6]uril-based [3]rotaxane supramolecular ionic liquid as a green and excellent corrosion inhibitor for the chemical industry," *Colloids Surf. A*, vol. 633, p. 127837, 2022.
[9] R. Hsissou *et al.*, "Trifunctional epoxy polymer as corrosion inhibition material for carbon steel in 1.0 M HCl: MD simulations, DFT and complexation computations," *Inorg. Chem. Commun.*, vol. 115, p. 107858, 2020.
[10] J. Lv, L. Fu, B. Zeng, M. Tang, and J. Li, "Synthesis and acidizing corrosion inhibition performance of N-doped carbon quantum dots," *Russ. J. Appl. Chem.*, vol. 92, pp. 848–856, 2019.
[11] A. Jiemuratova, U. B. Pardayev, and J. Bobojonov, "Coordination interaction between anthranilic ligand and d-element salts during crystal formation: A structural and spectroscopic approach," *Mod. Sci. Res.*, vol. 4, no. 5, pp. 199–201, 2025.
[12] Z. S. Bobozhonov, A. A. Sidikov, and Z. S. Shukurov, "Study of solubility of $CH_3COOH–CO(NH_2)_2–H_2O$ system," *J. Chem. Technol. Metall.*, vol. 58, no. 2, 2023.
[13] Zh. Sh. Bobozhonov *et al.*, "Solubility of components in aqueous systems including ethanol with carbamide and urea phosphate," *Eurasian Union Sci.*, no. 8-5, pp. 61–64, 2020.
[14] S. Xamdamova, U. B. Pardayev, and X. Kosimova, "Spectrophotometric analysis of 2-phenoxyethyldimethylbenzylammonium-2-oxynaphthoate and its correlation with antiparasitic activity," *Int. J. Med. Sci.*, vol. 1, no. 5, pp. 3–11, 2025.
[15] P. U. Xayrullo *et al.*, "Comparative analysis of thermal and thermochemical activation of bio-waste for carbon adsorbent production," *Conf. Mod. Sci. Pedagogy*, vol. 1, no. 3, pp. 646–652, 2025.
[16] I. Merimi *et al.*, "Metal corrosion inhibition by triazoles: A review," *Korroz.: Zashchita Mater.*, no. 3, pp. 17–36, 2023.
[17] U. B. Pardayev *et al.*, "The chemical basis for the development of new agrochemical preparations based on acrylonitrile," *Int. J. Med. Sci.*, vol. 1, no. 5, pp. 250–257, 2025.
[18] B. A. Smanov *et al.*, "Investigation of corrosion and scale inhibition efficiency using GPUSh inhibitor," *World Sci. Educ.*, no. 20, pp. 85–91, 2024.
[19] O. A. Kuchkarov *et al.*, "Investigation of particular parameters of a semiconductor ammonia gas analyzer," *IOP Conf. Ser.: Mater. Sci. Eng.*, vol. 862, no. 6, p. 062101, 2020.
[20] G. O. Sherzod-O'G'li *et al.*, "Comparative analysis of biochemical composition of green and yellowing leaves of 'Renet Simirenko' apple," *Sci. Educ.*, vol. 7, no. 2, pp. 47–54, 2026.
[21] G. S. Kholjigitov *et al.*, "Biochemical analysis of the effects of nitrogen, phosphorus, and potassium on photosynthetic pigments and metabolic processes in apple leaves," *Int. Conf. Platform*, no. 3, pp. 7–12, 2026.
[22] I. Elyos and N. Mokhinur, "Comprehensive analysis of the supramolecular complex structure: Inhibiting the β-SDOFDA effect of temperature through concentration and infrared spectroscopy," *Nauchnyi Redaktor*, p. 27, 2023.